

# Electrochemical Impedance Spectroscopy Investigations of Steel Corrosion in Acid media in the presence of Thiophene Derivatives

S. Ben Aoun<sup>1,\*</sup>, M. Bouklah<sup>2,\*\*</sup>, K.F. Khaled<sup>3</sup>, B. Hammouti<sup>2,\*\*\*</sup>

<sup>1</sup> Department of Chemistry, Faculty of Science, Taibah University, PO Box 30002 Al-Madinah Al-Munawarah, KSA.

<sup>2</sup> Laboratory of Applied Chemistry and Environment (LCAE), Faculty of Science, Mohammed Premier University, B.P. 717, M-6000 Oujda, Morocco

<sup>3</sup> Materials and corrosion laboratory (MCL), Chemistry Department, Taif University, P.O. 888, Taif, KSA.

\*E-mail: [sbenaoun@taibahu.edu.sa](mailto:sbenaoun@taibahu.edu.sa)

\*\*E-mail: [boukmmm@yahoo.fr](mailto:boukmmm@yahoo.fr)

\*\*\*E-mail: [hammoutib@gmail.com](mailto:hammoutib@gmail.com)

Received: 6 April 2016 / Accepted: 19 June 2016 / Published: 7 August 2016

---

Reinforcing steel corrosion behavior in the presence of 2-(thiophen-3-yl)ethanamine (3ET) and 2-(thiophen-2-yl)ethanamine (2ET) was studied using Electrochemical impedance spectroscopy. Both pit growth and corrosion of steel were inhibited with either compound present in the corroding medium. (EIS) measurements permitted the investigation of concentration, immersion time and the applied potential effects. Inhibition efficiencies up to ca. 86.22% and ca. 86.51% were achieved in the presence of  $5 \times 10^{-3} \text{M}$  (2ET) and (3ET), respectively.

---

**Keywords:** EIS, thiophene, inhibition, steel, potential of zero charge (PZC), Equivalent circuit

## 1. INTRODUCTION

Steel is regarded, world widely, as one of the most important materials that is used in almost each and every aspect of human life. This ranges from constructions and transport manufacturing industry, to protective footwear and electronic appliances and from giant aircrafts to fine surgical tools. As a consequence, a drastic number of steel grades exist worldwide, having various chemical structures and formulae and with specific systems of numbering that are used in different countries to categorize the tremendous number of existing steel alloys. Moreover, the steel user has a great deal of options as a consequence of the available shapes, microstructures, surface finishes, heat treatments and

forming conditions. Yet, all available types of steel can still be classified into a small number of groups depending on chemical composition, surface conditions, applications and shapes. The widespread problems of steel corrosion attracted a considerable attention. For this, inhibitors represent one of the most widely used corrosion protection techniques. Several studies, especially in acids, investigated the inhibiting activity on the steel corrosion of N-containing organic compounds [1–11] with most of them acting by adsorption onto the metal surface [4]. Thermodynamics models are important tools in mechanistic studies of corrosion inhibitors and a suggested one for the process of adsorption onto metal surface has been proposed [12,13]. It is well reported that efficient inhibitors contain unshared electron pairs, present on either sulfur or nitrogen, as well as p-electrons in their structures that would occupy the iron's d-orbitals. The chemical adsorption onto the steel surface may occur, by means of electrons transference, leading to the suppression of corrosion with the formed protective layer.

### 1.1. Steel corrosion electrochemistry

The corrosion of iron (or steel) is essentially an electrochemical process.

At the anode:



And while iron is corroding, the rate of reaction is usually controlled by the cathodic process.

In this respect, a variety of cathodic reactions are encountered and the main ones are:

Hydrogen reduction/evolution reaction:



Oxygen reduction reaction, either in:

Acid medium:



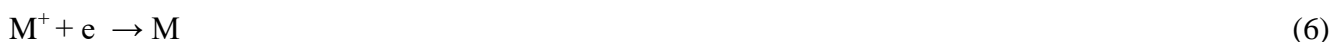
Or in neutral or basic media:



Metal ions reduction reaction:



Metal ions electrodeposition:



All these cathodic reactions consume electrons. The evolution of hydrogen gas is a very common process since most investigations are done in acid media. The same goes for oxygen reduction reaction which is common to aerated aqueous solutions. However, the reduction of metal ions and/or their electrodeposition are much less common.

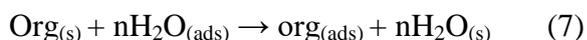
As those cathodic and anodic processes are interrelated, it is obvious that the whole corrosion process would be controllable by controlling either processes rate. For instance, protecting the surface of the metal with painting or through the formation of other protecting film, will affect both anodic and cathodic reactions rates which will be significantly decelerated which in turn retards the corrosion process.

On the other hand, the metal corrosion, and by consequence its corrosion inhibition processes depends tremendously on the electrolyte anionic composition.

### 1.2. Corrosion protection by inhibitors

A corrosion inhibitor decreases the corrosion rate when added to the corrosive environment in a suitable concentration. Such a compound operates through interfering with the cathodic and/or the anodic reactions and a great deal of inhibitors are organic compounds.

Corrosion inhibition is generally assumed to proceed by metal-solution interfacial adsorption and it is well established that the difference between the corrosive media and the corroding surface potentials is due to the unequal interfacial charges distribution. This causes changes in electrical double layer structure and properties as a consequence of the interactions driven by ions or corrosion inhibitor neutral molecules. Surface- adsorbed water molecules that are in contact with the corrosive solution take part in this process, as well. According to Bockris [14], one can describe the organic substance adsorption on a metal-solution interface by a displacement reaction as per the equation:



The desorbed number of molecules of water from the surface of the corroding metal per adsorbed molecule of inhibitor ( $n$ ) is independent of both the electrode charge and coverage [14]. Obviously, this number depends on the adsorbed organic molecules cross-sectional area. This adsorption takes place for the simple reason that the surface/water molecules interaction energy is lower than the inhibitor/metal surface one.

According to Lorenz and Mansfeld [15], corrosion inhibitory effects are of three types: (i) a geometric induced blocking effect of adsorbed inhibiting species onto the metal surface, (ii) a blocking of the active sites on the metal surface by adsorbed inhibiting species and (iii) the inhibitor electrocatalytic effect. Cao [16] reported that the first type originates from a decrease of the corroding metal reactive area, while the others are due to the elevation of the activation energies of the corrosion process. As a consequence, there should be different interpretations of the obtained electrochemical data originating from each of those modes.

On the other hand, thiophene-based compounds received special interest for their wide applicability. For instance, such compounds act as precursors for several high therapeutical potential like in hypertension, osteoporosis, AIDS, Alzheimer's disease and cancer [17–25]. Additionally, they have been recently applied to the inhibition of copper and mild steel corrosion [26–36]. Some very promising results were obtained with 2-(thiophen-3-yl)ethanamine (3ET) and 2-(thiophen-2-yl)ethanamine (2ET) [26] on steel corrosion in sulfuric acid (i.e. inhibition efficiency of ca. 96% for 3ET and ca. 98% for 2ET with a concentration of  $5 \times 10^{-3} \text{M}$  in either cases).

The current investigation aims to elucidate the effect of concentration, immersion time and potential for 2-(thiophen-3-yl)ethanamine (3ET) and 2-(thiophen-2-yl)ethanamine (2ET) on the inhibitory effects of the dissolution of steel in a 0.5M  $\text{H}_2\text{SO}_4$  solution using electrochemical impedance spectroscopy (EIS) measurements.

1.3. Theory

A big variety of electrochemical methods can be utilized for corrosion study and to investigate the efficiency of chemical inhibitors. In this respect, a quite powerful technique is the (EIS) owing to the great deal of information it provides such as the polarization resistance ( $R_p$ ) and double layer capacitance ( $C_{dl}$ ). For instance, monitoring these parameters permits to gain an insight on the investigated corrosion process kinetics [37]. For some cases, the obtained results at the corrosion potential ( $E_{Corr}$ ) show a semicircle with its center depressed below the real axis and the corresponding fitting circuit comprises a parallel resistance and capacitance [38] as shown in Fig. 1. It is noteworthy that better fitting of the depressed semicircles were reported when replacing the capacitance with a constant phase element (CPE) [39] the impedance of which is:

$$Z = Z_0 (j\omega)^{-n} \tag{8}$$

with n ranging from 0 to 1, according to the represented element in the circuit,  $\omega$  is the pulsation and j a complex number.

A depressed semicircle complex impedance  $Z(j\omega)$  can be expressed as:

$$Z = R_S + \frac{R_P}{1+(j\omega C_{dl} R_P)^{-n}} \tag{9}$$

For an ideal capacitor, the exponent n equals 1 and is a unitless parameter. This exponents deviates from unity in most of the real systems due to the uneven current distributions on the electrode surface as a consequence of surface roughness or other effects.

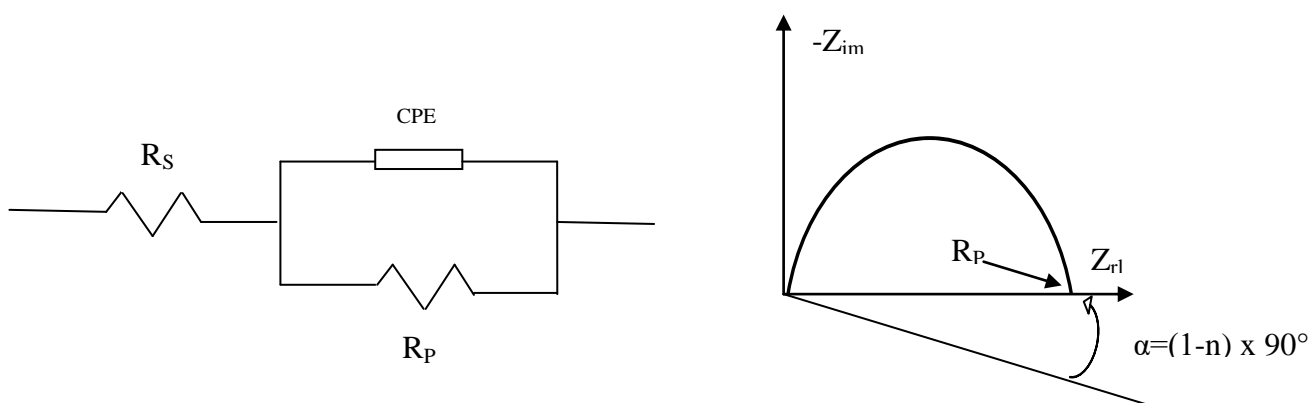


**Figure 1.** Equivalent electrical circuit with a constant phase element (CPE) and diagram of the Nyquist spectroscopy.

For an ideal behavior (i.e.  $n=1$ ), the term  $(j\omega C_{dl} R_P)^{-n}$  will reduce to  $(j\omega C_{dl} R_P)^{-1}$ , where  $C_{dl}$  is the interfacial double-layer capacitance, and this is indicative of the inhomogeneity of the metal surface [40]. Values that are slightly above 0.5 indicate high inhomogeneity while a value of unity reveals a smooth surface. The surface fractal dimension has been associated with the degree of inhomogeneity [41–42] and can be determined by considering the depression degree of the Nyquist diagram semicircle according to the equation [43]:

$$n = \frac{1}{D_S - 1} \tag{10}$$

$D_s$  denotes the surface fractal dimension, and has values between 2 and less than 3 for completely smooth and rough surfaces, respectively. A verification of this behavior was reported by Mac Rae et al. [44] who proved that measurements of the (EIS) yields the electrode's fractal dimension.

$$Z(P) = \frac{(R_s + R_t)[1 + \frac{R_s R_t}{R_s + R_t} C_{dl} P]}{1 + R_t C_{dl} P} = K \cdot \frac{1 + \tau_2 P}{1 + \tau_1 P} \tag{11}$$

where  $K=(R_s+R_t)$ ;  $\tau_1=R_t C_{dl}$ ;  $\tau_2=R_s R_t C_{dl} / (R_s+R_t)$ ;  $\omega_{c1}=2\pi f_{c1}=1/\tau_1$ ;  $\omega_{c2}=2\pi f_{c2}=1/\tau_2$ ;  $P=j\omega$   
 $\tau_1$  and  $\tau_2$  time constants correspond of pulsations  $\omega_{c1}$  and  $\omega_{c2}$ . (CPE =  $C_{dl}$  where  $n=1$ )  
 $\lim_{f \rightarrow +\infty} |Z| = R_s$  and  $\lim_{f \rightarrow 0} |Z| = R_s + R_t$

$$Z = R_s + \frac{R_t}{1 + jR_t C_{dl} \omega} = R_s + \frac{R_t}{1 + (R_t C_{dl} \omega)^2} - j \frac{R_t^2 C_{dl} \omega}{1 + (R_t C_{dl} \omega)^2} \tag{12}$$

$$X = R_s + \frac{R_t}{1 + (R_t C_{dl} \omega)^2} \quad \text{and} \quad Y = j \frac{R_t^2 C_{dl} \omega}{1 + (R_t C_{dl} \omega)^2} \tag{13}$$

$$[X - (R_s + \frac{R_t}{2})]^2 + Y^2 = (\frac{R_t}{2})^2 \tag{14}$$

This is the equation of a circle of a radius ( $R_t/2$ ) and a center ( $R_s+R_t/2, 0$ ). The Impedance imaginary part values are negative. The circle of equation (14) reduces to a semicircle, which is confirmed by the Nyquist representation. The phase of the impedance is given by the following expressions:

$$\Phi_Z(\omega) = \text{Arg}[Z(\omega)] = \text{Arctg} [\text{Im } Z(\omega) / \text{Re } Z(\omega)] \tag{15}$$

$$\Phi_Z(\omega) = -\text{Arctg} \frac{R_t^2 C_{dl} \omega}{[(R_s + R_t) + R_s R_t^2 C_{dl}^2 \omega^2]} \tag{16}$$

When  $\omega \rightarrow 0$  (i.e. at a low frequency)  $\Phi_Z(\omega) \rightarrow 0$

When  $\omega \rightarrow \infty$  (i.e. at a High frequency)  $\Phi_Z(\omega) \rightarrow 0$

## 2. EXPERIMENTAL

### 2.1. Materials

A carbon steel rod (Al 0.01, Mn 0.05%, S 0.05%, P 0.09%, C 0.21%, %Si 0.38%, Fe remainder) was utilized to prepare the testing specimens. Cut cylindrical discs were tied with Teflon on a glass tube holder with an exposed  $1\text{cm}^2$  surface area. Prior to immersion in corrosive media, the prepared specimen was firstly abraded with 1200 grit sandpaper and washed thoroughly with acetone then doubly-distilled water. The corrosive media consisted of a 0.5M  $\text{H}_2\text{SO}_4$  solution that was prepared from a stock solution of analytical grade ( $\text{H}_2\text{SO}_4$ , 98%). All experiments were conducted at room temperature under magnetic stirring.

## 2.2. Inhibitors compounds

Fig. 2 shows the chemical structures of the studied thiophene derivatives (i.e. 2-(thiophen-3-yl)ethanamine (3ET) and 2-(thiophen-2-yl)ethanamine (2ET)).



**Figure 2.** Structure of the investigated thiophene derivatives.

## 2.3. Electrochemical Impedance Spectroscopy (EIS)

All EIS experiments were conducted in aerated acid solution at  $E_{\text{corr}}$  using a computer-controlled Tacussel electrochemical system (model Voltalab PGZ 100). The working electrode consisted of the exposed steel surface (ca. 1 cm<sup>2</sup>), and was used along with a platinum auxiliary electrode and a saturated calomel electrode (SCE) reference electrode. After 30 min exposure time, the steady-state current was determined and a sine wave excitation voltage (10 mV peak to peak) was superimposed at frequencies ranging from 100 kHz to 10 MHz. The obtained results were reported as Nyquist plots.

## 3. RESULTS AND DISCUSSION

### 3.1 Effect of the inhibitor's concentration

Figure 3 displays the Nyquist plots for steel in a 0.5M H<sub>2</sub>SO<sub>4</sub> solution containing varying concentrations of 2-(thiophen-3-yl)ethanamine (3ET) and 2-(thiophen-2-yl)ethanamine (2ET). The observed one semicircle is an indication that steel dissolution comprises of a single process of charge transfer that remains unaffected after addition of inhibitors molecules. The high frequencies inductive loop reveals the relaxation of adsorbed species occurring at metal-corrosive solution interface while the typical semicircle with a slight depression and a center located below the real axis evidences inhomogeneties of solid electrodes, like some degree of roughness and/or others [45, 46].

Table 1 displays the derived charge transfer resistance ( $R_t$ ) and double layer capacitance ( $C_{dl}$ ) values. The former shows an increase from ca. 30 to ca. 217.8  $\Omega$  while the latter decreased from ca. 103 to ca. 40.9  $\mu\text{Fcm}^{-2}$  for 2ET, whereas  $R_t$  increased from ca. 30 to ca. 222.4  $\Omega$  and  $C_{dl}$  decreased from ca. 103 to ca. 45.92  $\mu\text{Fcm}^{-2}$  for 3ET.

The commonly used equivalent circuit in fitting the results shown in Fig. 3, with a single time constant, is displayed in Fig. 4. However, to accommodate the slightly depressed semicircles a two-

time constants process is introduced: (i) the first one at high frequencies pertains to the relaxation of Fe<sub>2</sub>O on the metal surface; and (ii) the second, at low frequencies, is related to the dissolved oxygen diffusion.

The degree of corrosion resistance is evidenced by the polarization resistance (R<sub>p</sub>) that is given by [47]:

$$R_p = \lim_{\omega \rightarrow 0} R_s \{Z_f\}_{E=E_{corr}} \tag{17}$$

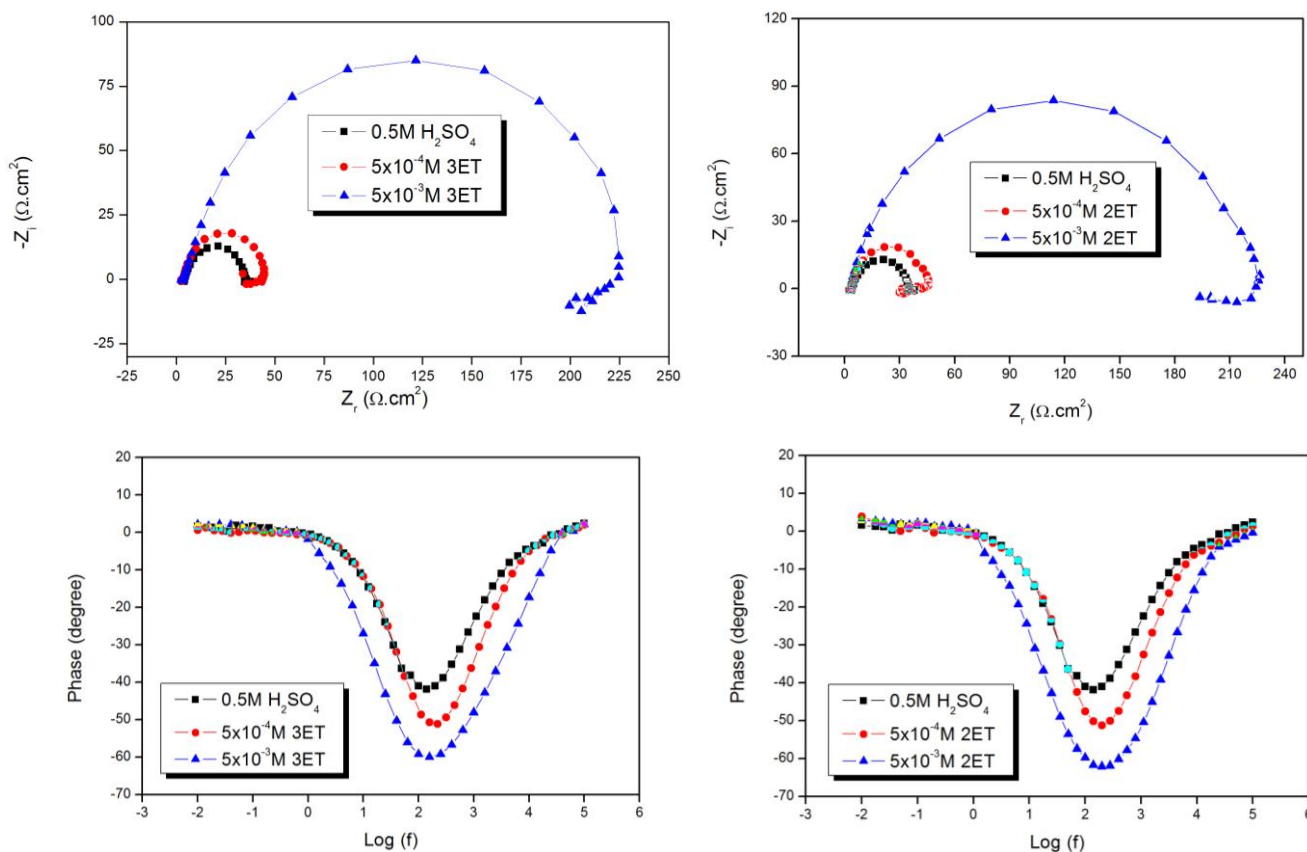
Re{Z<sub>f</sub>} being the complex faradic impedance (Z<sub>f</sub>) real part and ω represents the frequency-dependant angular velocity (ω=2Πf). The values are listed in Table 1

The inhibition efficiency was calculated as [48]:

$$E\% = \frac{R_t^{inh} - R_t}{R_t^{inh}} \times 100 \tag{18}$$

R<sub>t</sub><sup>inh</sup> and R<sub>t</sub> denote the charge transfer resistance value in corrosive media with and without inhibitors, respectively. For both compounds, the (E%) increased proportionally with inhibitors' concentrations (cf. Table 1).

It is clearly shown that both 2ET and 3ET are very effective for the inhibition of steel corrosion in the present work conditions with increasing R<sub>p</sub> values with increasing inhibitor concentration. These observations agree very well with the results shown from polarization and weight loss techniques, reported previously [26]. In addition, figure 3 shows that with increasing inhibitor concentration, the phase angle increases and approaches 90° for both 2ET and 3ET suggesting a resistive to capacitive system “switching” as a consequence of a protecting layer adsorbed onto the metal surface indicating that the inhibitor diffuses through mortar leading to corrosion activity hindering on the steel surface.



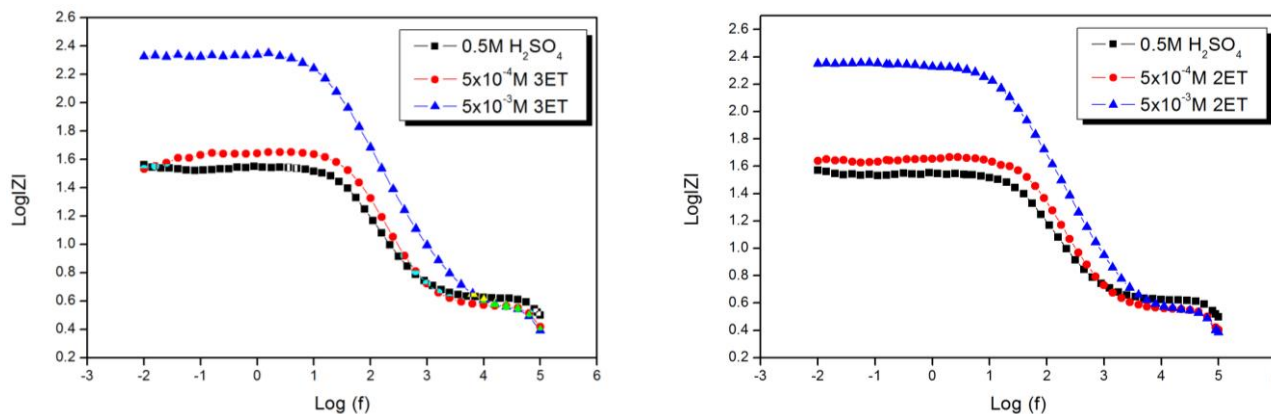


Figure 3. Nyquist and Bode plots for steel in 0.5M H<sub>2</sub>SO<sub>4</sub> at various concentrations of 3ET and 2ET.

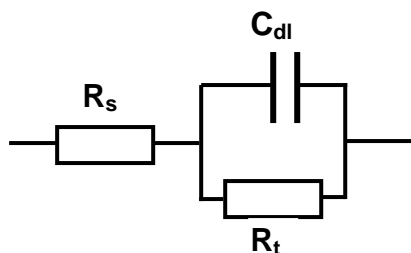


Figure 4. The equivalent electrical circuit used in the fitting of the experimental results.

Table 1. Impedance parameters and corresponding inhibition efficiencies for the corrosion of steel in 0.5M H<sub>2</sub>SO<sub>4</sub> with and without inhibitors.

	C(M)	E <sub>corr</sub> (mV/SCE)	R <sub>s</sub> (Ω)	R <sub>t</sub> (Ω)	R <sub>p</sub> (Ω)	C <sub>dl</sub> (μF.cm <sup>-2</sup> )	f <sub>max</sub> (Hz)	E %
blank	0.5M H <sub>2</sub> SO <sub>4</sub>	-465	4.86	30	25.14	103	51.50	–
2ET	5x10 <sup>-4</sup>	-446	3.58	42.53	38.95	74.83	50.00	29.46
	5x10 <sup>-3</sup>	-441	3.52	217.8	214.28	40.90	17.85	86.22
3ET	5x10 <sup>-4</sup>	-478	3.11	43.37	40.26	91.74	40.00	30.82
	5x10 <sup>-3</sup>	-462	3.47	222.4	218.93	45.92	15.82	86.51

### 3.2 Effect of the immersion time

The Nyquist plots of steel in a 0.5M H<sub>2</sub>SO<sub>4</sub> solution given in Fig. 5 show increasing semicircles with increasing time up to 3h as a consequence of gradually changing kinetics of the corrosion process, and this could be related to a growing protective scale with growing protection [49–50]. Yet, an abrupt decrease of the impedance magnitude was observed after 3 hours.

Table 2 lists the results of the best experimental data fitting in terms of equivalent electrical circuit elements. A relatively small decrease of solution resistance (R<sub>s</sub>) values was observed from

4.86Ω to 4.12 Ω for immersion times of 0.5h and 10h, respectively, owing to increasing ions concentration as a result of increasing steel dissolution. Whereas, this induces a charge transfer resistance ( $R_t$ ) increase which reveals an impeded charge transfer process, as a result of the shrinking of uncovered steel area [51]. Similarly, the double layer capacitance ( $C_{dl}$ ) values at intermediate characteristic frequencies (10mHz–100KHz), increased with increasing time of immersion. Yet, they remain in the typical order of magnitude for a double–layer capacitance [52–54].

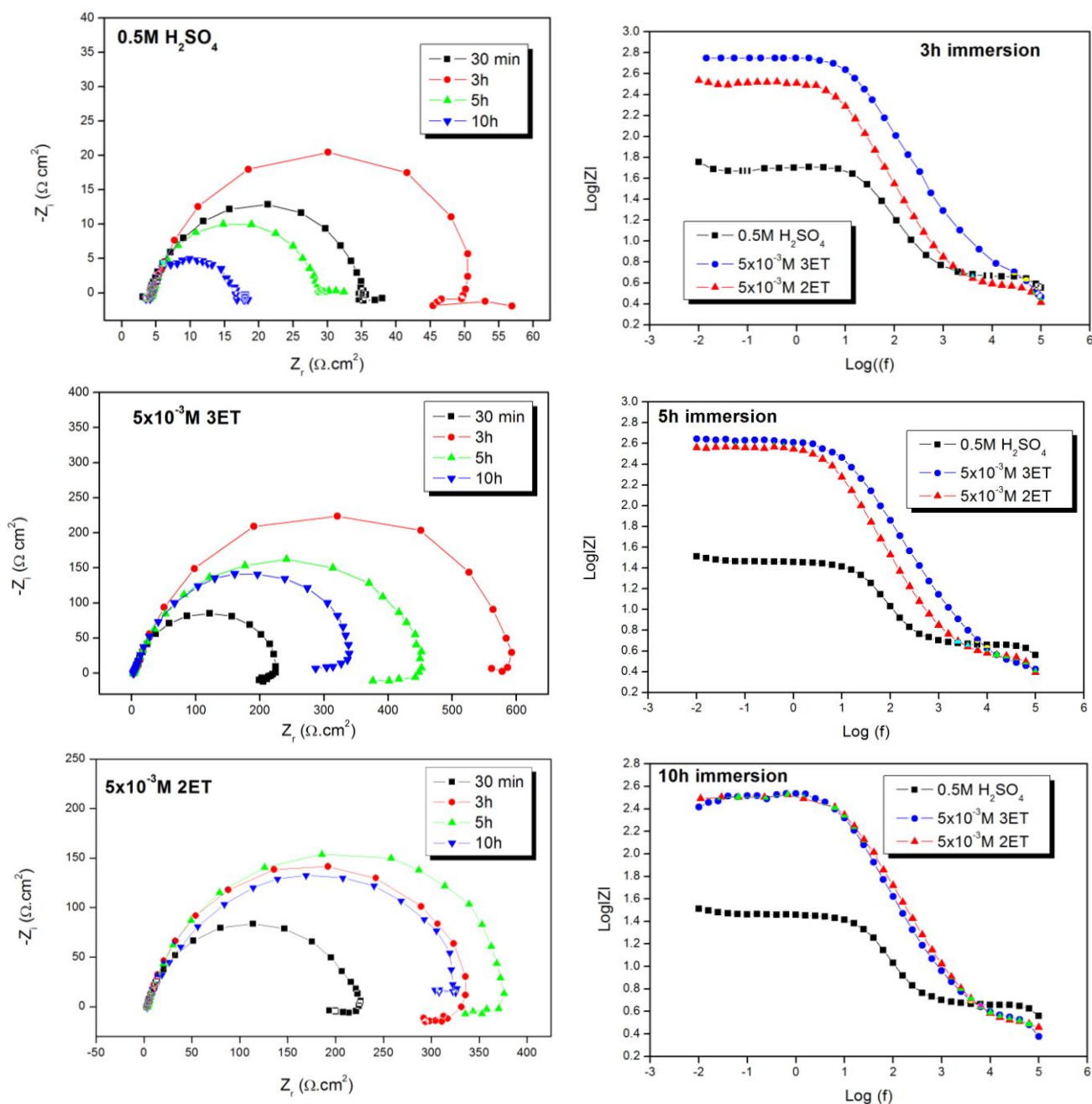


**Figure 5.** Nyquist and Bode plots at different immersion times with and without  $5 \times 10^{-3}$ M thiophene derivatives.

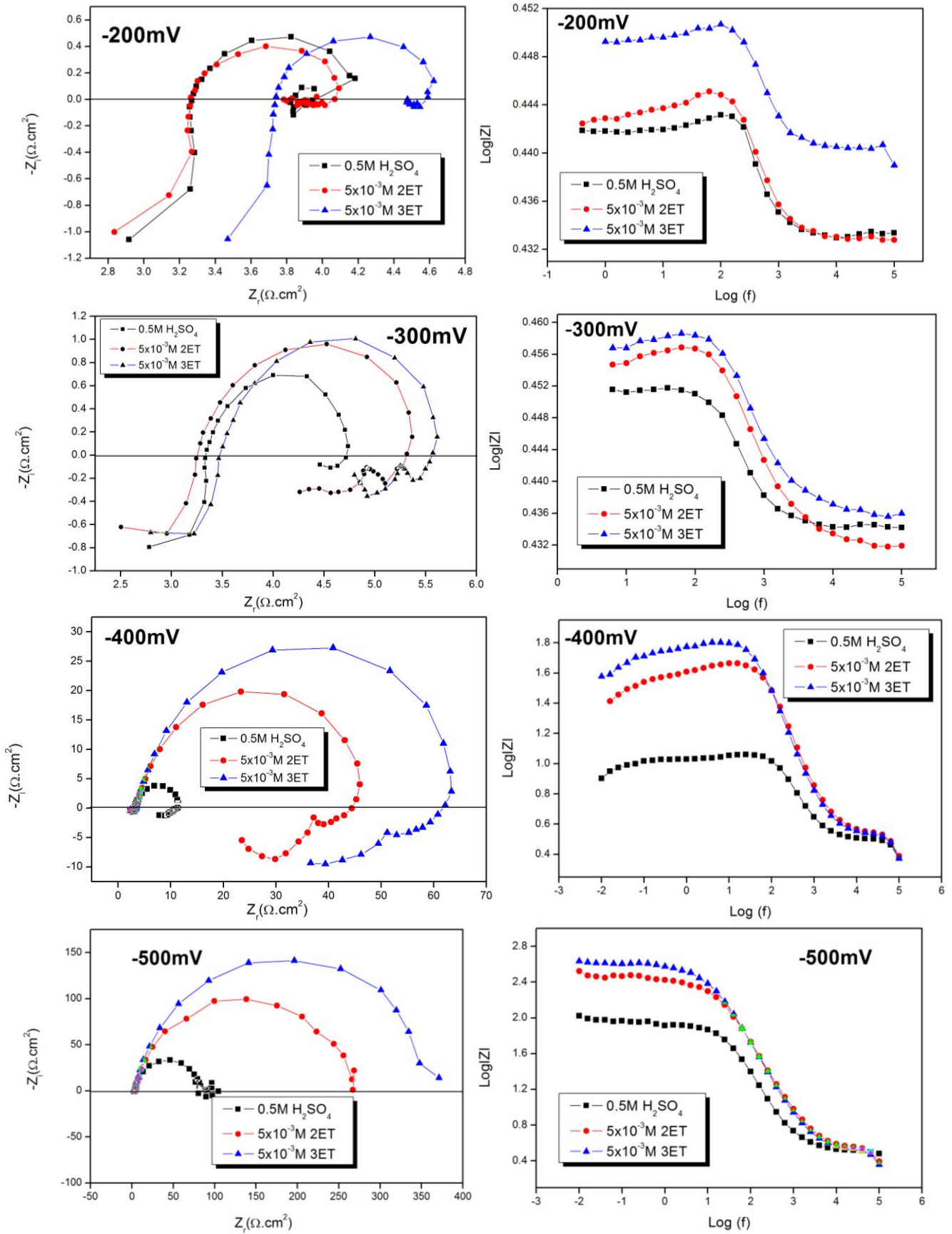
**Table 2.** Impedance measurements and inhibition efficiency for steel in 0.5M H<sub>2</sub>SO<sub>4</sub> containing different concentrations of 3ET and 2ET at 25°C

inhibitors	Time (h)	R <sub>s</sub> (Ω)	R <sub>t</sub> (Ω)	C <sub>dl</sub> (μF.cm <sup>-2</sup> )	f <sub>max</sub> (Hz)	E%
H <sub>2</sub> SO <sub>4</sub> 0.5M	0.5	4.86	30	103	51.50	–
	3	4.58	47.92	118.2	25	–
	5	4.55	24.18	207.9	32	–
	10	4.12	14.02	270.28	42	–
3ET	0.5	3.47	222.4	45.92	15.82	86.51
	3	4.58	586.7	19.31	15.82	91.83
	5	3.03	415.9	30.61	10	94.18
	10	3.44	349.5	57.37	7.93	95.99
2ET	0.5	3.52	217.8	40.90	17.85	86.22
	3	3.98	350.5	72.74	6.32	86.33
	5	3.56	366.1	68.67	6.32	93.39
	10	3.23	348.7	45.64	10	95.97

### 3.3 Effect of the potential

Fig.6 presents the impedance spectra of protected and unprotected steel in deaerated 0.5M H<sub>2</sub>SO<sub>4</sub> solution at different potentials. In the anodic domain,  $E > E_{\text{corr}} = -461\text{mV}$ , (i.e.  $E = -200\text{mV}$ ,  $E = -300\text{mV}$  and  $E = -400\text{mV}$ ), the observed semi-circles give an indication of a protecting layer formation onto the corroding steel surface. One can note the existence of a capacitive single loop and a subsequent inductive loop located at high and at low frequencies, respectively, in accordance to literature [55,56]. The former is attributable to the corrosion process charge transfer along with an oxide layer formation while the latter is very often attributed to either species relaxations on the surface oxide layer [57] or to this layer's stabilization by intermediate corrosion products adsorbed on the electrode surface [58]. A model of the fitting circuit is given in Fig.7, where the inductance (L) and the resistance (R<sub>ind</sub>) are correlated with intermediate processes at low frequencies, while (R<sub>p</sub> + R<sub>ind</sub>) identifies with a charge transfer resistance (R<sub>t</sub>) [55,58].

A single semicircle was obtained in the cathodic domain,  $E < E_{\text{corr}} = -461\text{mV}$ , (i.e.  $E = -500\text{mV}$ ,  $E = -600\text{mV}$ ,  $E = -700\text{mV}$  and  $E = -800\text{mV}$ ), with similar impedance spectra showing a one-time constant depressed semicircles. This observed behavior fits well to the equivalent electrical circuit displayed in Fig. 1 featuring a combination of parallel constant phase element (CPE) and polarization resistance (R<sub>p</sub>) in series with a solution resistance (R<sub>s</sub>), similarly with reported results for acidic steel corrosion [59–61]. In the presence of thiophene-based inhibitors, an eye-catching feature is the increase in the semicircles diameters. It is worth mentioning that, for a typical Randles equivalent circuit, the Nyquist impedance plot extrapolation in low frequencies domain gives the polarization resistance (R<sub>p</sub>) value which in this case equals the diameter of the semicircle. The metal surface roughness is represented by the constant phase element (CPE) and the fractal dimension of that surface is calculated from depression angle.



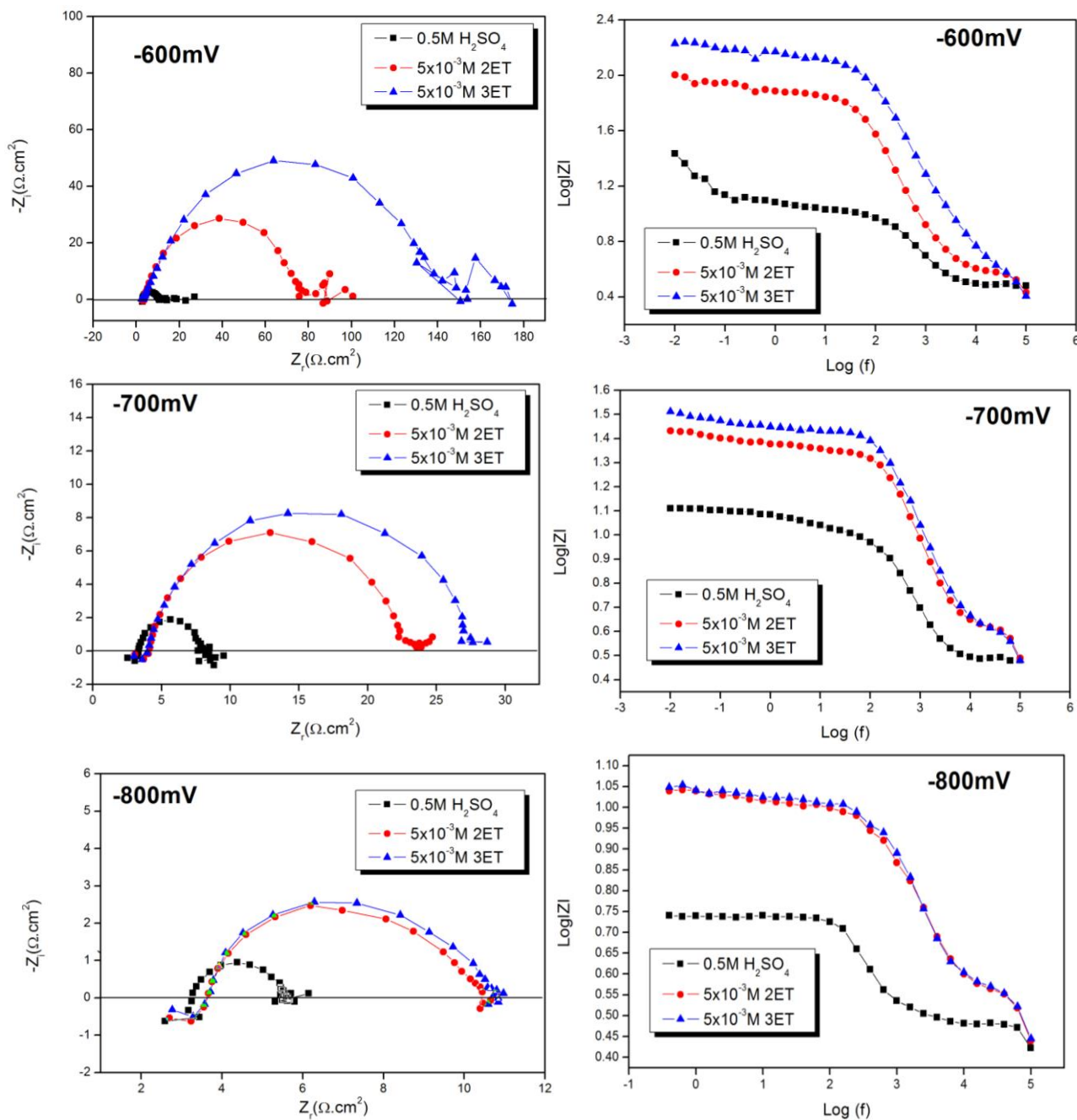


**Figure 6.** Nyquist and Bode plots of steel at different anodic and cathodic potential domains with and without  $5 \times 10^{-3}$  M thiophene derivatives.

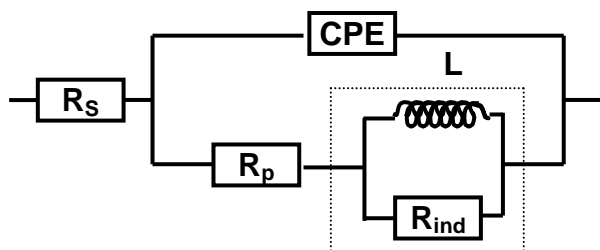


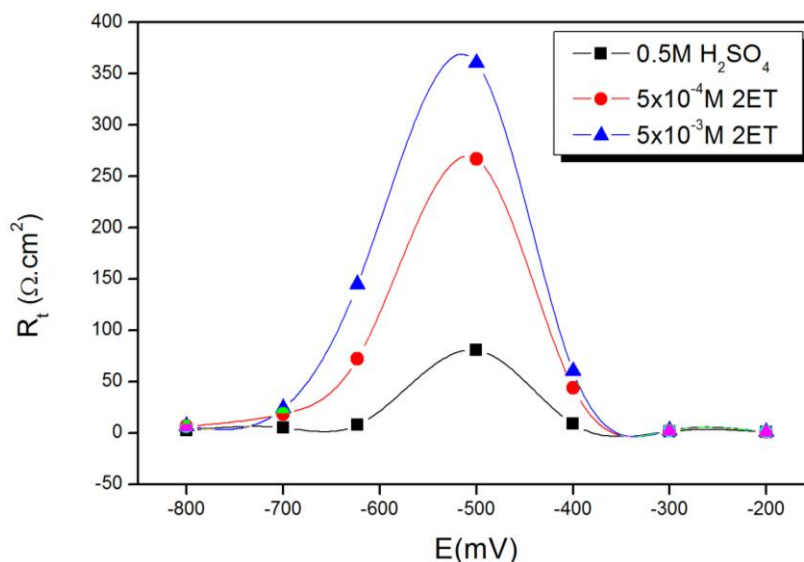
**Figure 7.** Electrical circuit model used for the fitting of the experimental impedance data.

**Table 3.** Electrochemical parameters of impedance for steel in 0.5M H<sub>2</sub>SO<sub>4</sub> without and with addition of various concentrations of thiophene derivatives.

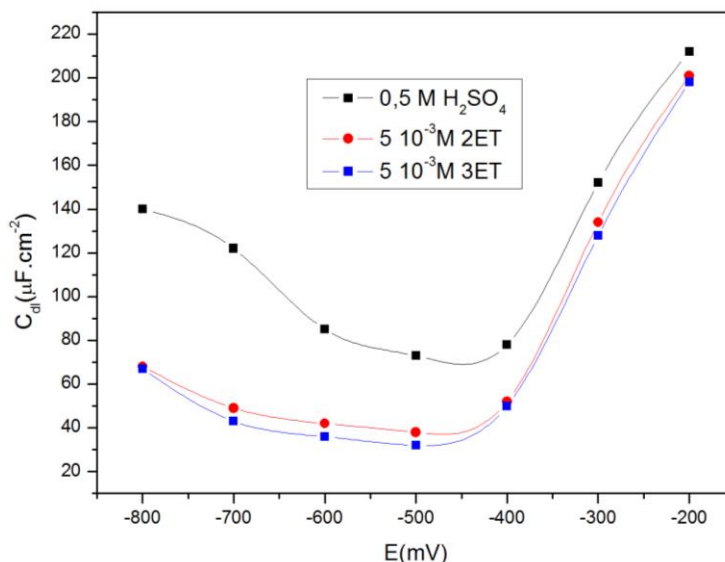
E (mV)		-800	-700	-600	-500	-400	-300	-200
R <sub>s</sub> (Ω)	0.5M H <sub>2</sub> SO <sub>4</sub>	3.25	3.33	3.06	3.32	3.17	3.33	3.62
	2ET	3.26	4.16	3.43	3.07	3.50	3.24	3.26
	3ET	3.70	3.24	2.54	3.41	3.43	3.50	3.74
R <sub>t</sub> (Ω)	0.5M H <sub>2</sub> SO <sub>4</sub>	2.31	4.89	7.70	80.78	8.65	1.38	0.92
	2ET	6.31	18.64	72.38	266.8	43.7	2.14	0.82
	3ET	6.66	23.98	137.9	360.3	60.22	2.16	0.86
C <sub>dl</sub> (μF.cm <sup>-2</sup> )	0.5M H <sub>2</sub> SO <sub>4</sub>	140	122.1	85.3	73.56	78.8	152	212
	2ET	68	49	42	38	52	134	201
	3ET	66.9	43.12	36.5	32	50	128	198
f <sub>max</sub> (Hz)	0.5M H <sub>2</sub> SO <sub>4</sub>	492	266.5	242	26.78	234	758	816
	2ET	371	348.5	52.35	15.69	70	555	966
	3ET	357.3	153.9	31.62	13.8	52.85	575.6	934
E%	2ET	63.42	73.86	89.36	69.72	80.18	35.32	9.24
	3ET	65.36	79.6	94.41	77.58	85.62	35.62	13.88

Table 3 lists the Nyquist plots/Bode diagrams-derived impedance parameters (data extracted from Fig.6), and shows an inhibition efficiency (E%) increase with the potential in the cathodic domain followed by a decrease in the anodic domain, for both 2ET and 3ET. Similar results were reported in literature for quinoxaline derivatives [62].

An AC impedance investigation permitted to define the potential of zero charge (PZC) and the plots of R<sub>t</sub> and C<sub>dl</sub> values at each applied potential are shown in Figs. 8 and 9, respectively. The obtained parabolas show a minimum at ca. -492mV in the blank solution against ca. -505mV and ca. -514mV for 3ET and 2ET, respectively.



**Figure 8.** Plots of R<sub>t</sub> vs. applied electrode potential with and without 5×10<sup>-3</sup>M thiophene derivatives.



**Figure 9.** Plots of  $C_{dl}$  vs. applied electrode potential with and without  $5 \times 10^{-3} \text{ M}$  thiophene derivatives.

Here we would like to point out the following three situations regarding the possibly adsorbed species onto steel surface:

1. In the case of a positively charged surface, with respect to PZC: Firstly, sulfate ( $\text{SO}_4^{2-}$ ) ions adsorb on the surface of the metal. Secondly, these adsorbed ions attract the cationic forms of the thiophene inhibitor along with the protonated molecules of water. Consequently, the formed triple layer with a close-packed structure would inhibit iron from entering into the solution.

2. In the case of a negatively charged surface, with respect to PZC, the cationic forms of the thiophene inhibitors along with the protonated molecules of water would directly adsorb onto the metal surface. Consequently, an increasing metal surface negative charge enhances the adsorption of 3ET and 2ET while their concentrations in the solution decreases.

3. At the PZC exactly, the metal surface is not charged and therefore no ionic adsorption occurs. A physical adsorption of few thiophene molecules might occur by means of  $\pi_p$  orbitals onto the steel surface (presenting vacant  $\pi_d$  orbitals) causing a slight decrease in thiophene concentrations.

#### 4. CONCLUSION

From the EIS investigations of the steel corrosion inhibition process at open circuit potential (OCP) in a 0.5 M  $\text{H}_2\text{SO}_4$  solution using thiophene derivatives inhibitors we conclude the following:

i- The Nyquist plots exhibited of a capacitive semicircle in the high frequencies regions and an inductive small loop in low frequencies.

ii- The inhibition efficiency of 3ET and 2ET for steel increases with increasing concentrations.

iii- The inhibition efficiency of 3ET and 2ET for steel increases with extended immersion time up to 3h, suggesting a gradually changing kinetics of the corrosion process. Yet, an abrupt decrease of the impedance magnitude was observed after 3 hours.

iv- The AC impedance-calculated the potential of zero charge (PZC) revealed that the values of the charge transfer resistance ( $R_t$ ) increased at potentials below the PZC then decreased above it, conversely  $C_{dl}$  decreased at potentials less positive than the PZC and then increased at higher potentials.

## References

1. P. Chatterjee, M.K. Benerjee, K.P. Mukherjee, *Ind. J. Technol.*, 29 (1991) 191.
2. M. Elachouri, M.S. Hajji, S. Kertit, E.M. Essassi, M. Salem, R. Coudert, *Corros. Sci.*, 37 (1995) 381.
3. B. Mernari, H. Elattari, M. Traisnel, F. Bentiss, M. Larenee, *Corros. Sci.*, 40 (1998) 391.
4. A. Mansri, B. Bouras, *Mor. J. Chem.* 2 (2014) 252.
5. A.S. Fouda, K. Shalabi, R. Ezzat, *J. Mater. Environ. Sci.*, 6 (2015) 1022.
6. A. Elkanouni, S. Kertit, A. Ben Bachir, *Bull. Electrochem.*, 12 (1996) 517.
7. O. Kassou, M. Galai, R.A. Ballakhmima, N. Dkhireche, A. Rochdi, M. Ebn Touhami, R. Tourir, A. Zarrouk, *J. Mater. Environ. Sci.*, 6 (2015) 1147.
8. S. Kertit, B. Hammouti, *Appl. Surf. Sci.*, 93 (1996) 59.
9. F. Bentiss, M. Lagrenee, M. Traisnel, J.C. Hornez, *Corros. Sci.*, 41 (1999) 789.
10. S. Ben Aoun, *Int. J. Electrochem. Sci.*, 8 (2013) 10788.
11. S. Ben Aoun, *Der Pharm. Chem.*, 5(2013) 294.
12. M. Bouklah, N. Benchat, B. Hammouti, S. Kertit, *Mater. Lett.*, 60 (2006) 1901.
13. T.P. Zhao, G.N. Mu, *Corros. Sci.*, 41 (1999) 1937.
14. J.O'M. Bockris, D.A.J. Swinkels, *J. Electrochem. Soc.*, 111 (1964) 736
15. W.J. Lorenz, F. Mansfeld, *proceeding of the 6th Symposium on European Inhibition of Corrosion*, University of Ferrara, Ferrara, 1985, p. 23.
16. C. Cao, *Corros. Sci.*, 38 (1996) 2073.
17. W. N. Neira, M. I. Rivera, G. Kohlhagen, M. L. Hursey, P. Pourquier, E. A. Sausville and Y. Pommier, *Mol. Pharmacol.*, 56 (1999) 478.
18. R. Villar, I. Encio, M. Migliaccio, M. J. Gil, V. Martinez–Merino, *Bioorg. Med. Chem.*, 12 (2004) 963.
19. M. B. Sahasrabudhe, M. K. Nerurkar, M. V. Nerurkar, B. D. Tilak, M. D. Bhavsar, *Br. J. Cancer*, 14 (1960) 547.
20. A.V. Kalinin, M. A. Reed, B. H. Norman, V. Snieckus, *J. Org. Chem.*, 68 (2003) 5992.
21. R. K Russell, J. B. Press, R. A. Rampulla, J. J. McNally, R. Falotico, J. A. Keiser, D. A. Bright, A. Tobia, *J. Med. Chem.*, 31 (1988) 1786.
22. W. C. McCormick, I. B. Abrass, *Lancet* 352 Supl. IV (1998) 6.
23. C. E. Stephens, T. M. Felder, J. W. Sowell, G. Andrei, J. Balzarini, R. Snoeck, E. De Clercq, *Bioorg. Med.Chem.*, 9 (2001) 1123.
24. J. B. Hudson, R. J. Marles, C. S. Breau, L. Harris, J. T. Arnason, *Photochem. Photobiol.*, 60 (1994) 591.
25. G. Guillet, J. Harmatha, T. G. Waddell, B. J. R. Philog<sub>ne</sub> and J. T. Arnason, *Photochem. Photobiol.*, 71 (2000) 111.
26. M . Bouklah, B . Hammouti, A . Aouniti, T. Benhadda, *Prog. in Org. Coa.*, 49 (2004) 225.
27. M.G. Medrano–Vaca, J.G. Gonzalez–Rodriguez, M.E. Nicho, M. Casales, V.M. Salinas–Bravo, *Electrochim. Acta*, 53 (2008) 3500.
28. M. Benabdellah, A. Aouniti, A. Dafali, B. Hammouti, M. Benkaddour, A. Yahyi, A. Ettouhami, *Appl. Sur. Sci.*, 252 (2006) 8341.
29. M. Benabdellah, A. Yahyi, A. Dafali, A. Aouniti, B. Hammouti, A. Ettouhami, *Arab. J. Chem.*, 4 (2011) 243.

30. A. Galal, N.F. Atta, M.H.S. Al-Hassan, *Mat. Chem. and Phys.*, 89 (2005) 38.
31. S. Issaadi, T. Douadi, A. Zouaoui, S. Chafaa, M.A. Khan, G. Bouet, *Corros. Sci.*, 53(2011) 1484.
32. P. Rajeev, A.O. Surendranathan, C.S.N. Murthy, L. John Berchmans, *J. Mater. Environ. Sci.*, 5 (2014) 440.
33. K. Bouhrira, A. Chetouani, D. Zerouali, B. Hammouti, A. Yahyi, A. Et-Touhami, R. Yahyaoui, R. Touzani, *Res. Chem. Int.*, 40 (2014) 569.
34. U. Leon-Silva, J.G. Gonzalez-Rodriguez, M.E. Nicho, V.M. Salinas-Bravo, J.G. Chacon-Nava, A. Martinez-Villafañe, *Corros. Sci.*, 52 (2010) 1086.
35. K.F.Khaled, N. A. Al-Mobarak, *Int. J. Electrochem. Sci.*, 7 (2012) 1045.
36. T.S. Lobana, Rekha, A.P.S. Pannu, G. Hundal, R.J. Butcher, A. Castineiras, *Polyhedron*, 26 (2007) 2621.
37. R. Cottis, S. Turgoose, *Electrochemical Impedance and Noise, NACE International, Houston, 1999.*
38. W.H. Mulder, J.H. Sluyters, *Electrochim. Acta*, 33(1988) 303.
39. M. Kissi, M. Bouklah, B. Hammouti, M. Benkaddour, *Appl. Surf. Sci.*, 252 (2006) 4190.
40. R. de Levie, *J. Electroanal. Chem.*, 261(1989) 1.
41. A. Popova, S. Raicheva, E. Sokolova, M. Christov, *Langmuir*, 12(1996) 2083.
42. L. Nykos, T. Pajkossy, *Electrochim. Acta*, 30 (1985) 1533.
43. W.H. Mulder, J.H. Sluyters, T. Pajkossy, L. Nyikos, *J. Electroanal. Chem.*, 285 (1990) 103.
44. G.A. McRae, M.A. Maguire, C.A. Jeffrey, D.A. Guzonas, C.A. Brown, *Appl. Surf. Sci.*, 191 (2002) 94.
45. M. Prabakaran, K. Vadivu, S. Ramesh, V. Periasamy, *J. Mater. Environ. Sci.*, 5 (2014) 553.
46. T. Paskossy, *J. Electroanal. Chem.*, 364 (1994) 111.
47. D.J. Loren, F. Mansfeld, *Corros. Sci.*, 21 (1981) 647.
48. S.-L. Li, Y.-G. Wang, S.-H. Chen, R. Yu, S.-B. Lei, H.-Y. Ma, D.-X. Lin, *Corros. Sci.*, 41 (1999) 1769.
49. J.L. Mora-Mendoza, S. Turgoose, *Corros. Sci.*, 44 (2002) 1223.
50. S. Nesic, K.-L.J. Lee, *Corrosion*, 59 (2003) 616.
51. J. Mar'in-Cruza, R. Cabrera-Sierra, M.A. Pech-Canul, I. Gonz'aleza, *Electrochim. Acta*, 51 (2006) 1847.
52. M. Sfaira, A. Srhiri, M. Keddami, H. Takenouti, *Electrochim. Acta*, 44 (1999) 4395.
53. K. Jüttner, W.J. Lorenz, M.W. Kendig, F. Mansfeld, *J. Electrochem. Soc.*, 135 (1988) 332.
54. L. Bousselmi, C. Fiaud, B. Tribollet, E. Triki, *Electrochim. Acta*, 44 (1999) 4357.
55. M. Ebrahimzadeh, M. Gholami, M. Momeni, A. Kosari, M.H. Moayed, A. Davoodi, *Appl. Surf. Sci.*, 332 (2015) 384.
56. L. Afrine, A. Zarrouk, H. Zarrok, R. Salghi, R. Tourir, B. Hammouti, H. Oudda, M. Assouag, H. Hannache, M. El Harti, M. Bouachrine, *J. Chem. Pharm. Res.*, 5 (2013) 1474.
57. S.S. Abd El-Rehim, H.H. Hassan, M.A. Amin, *Mater. Chem. Phys.*, 70 (2001) 64.
58. M. Gojic, R. Horvat, M. Metikos-Hukovic, *Proceedings of the Eighth European Symposium on Corrosion Inhibitors (8 SEIC)*, Univ. Ferrara, N.S. V, Suppl. N. 10, (1995) 97.
59. L. Elkadi, B. Mernari, M. Traisnel, F. Bentiss, M. Lagrenee, *Corros. Sci.*, 42 (2000) 703.
60. F. Bentiss, M. Traisnel, M. Lagrenee, *J. Appl. Electrochem.*, 31 (2001) 41.
61. K.F. Khaled, *Electrochim. Acta*, 48 (2003) 2493.
62. K. Benbouya, B. Zerga, M. Sfaira, M. Taleb, M. Ebn Touhami, B. Hammouti, H. Benzeid, E.M. Essassi, *Int. J. Electrochem. Sci.*, 7 (2012) 6313.